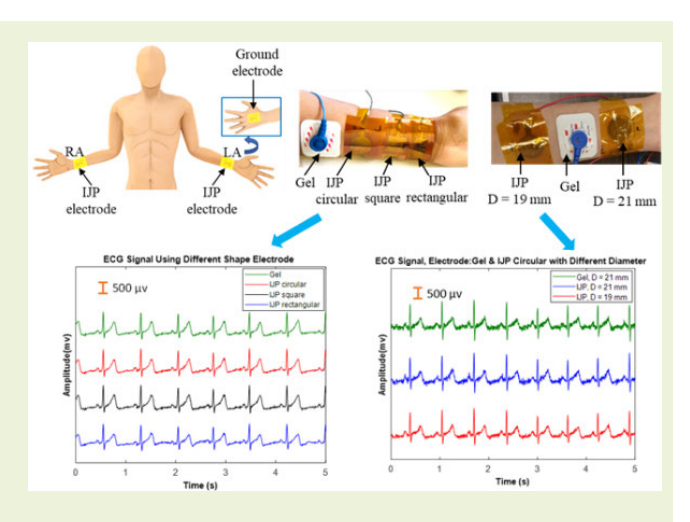


# Fabrication and Characterization of Inkjet Printed Flexible Dry ECG Electrodes

Mst Moriom Rojy Momota<sup>®</sup>, *Graduate Student Member, IEEE*, Bashir I. Morshed<sup>®</sup>, *Senior Member, IEEE*, Tamanna Ferdous, and Tomoko Fujiwara

Abstract—Commercial gel ECG electrodes have a limited lifetime of operation and metal dry electrodes are rigid and noisy. In this study, we developed flexible dry ECG electrodes in different shapes and sizes using an inkjet printing (IJP) technology. As an additive manufacturing technique, IJP provides the flexibility to personalize the shape and size of electrodes with rapid prototyping. IJP ECG electrodes were fabricated on flexible polyimide substrates using silver nanoparticle inks for the conductive layer and a custom polymer ink of poly(4-vinylphenol) (PVP) for the insulator layer. The maximum and minimum diameters of the electrodes were 21 and 9 mm, respectively. The thickness of IJP electrodes was 2  $\pm$  0.5  $\mu$ m. Various tests were performed for feasibility, including changing electrode position, and subject's activity such as resting, standing, and walking using IJP ECG electrodes simultaneous with clinical standard gel electrodes, which provides an accurate comparison. Compared to the gel electrode, the circular shape IJP electrode was more promising than rectangular and square shapes as it showed



more coherence to the gel electrode. IJP electrodes with different diameters were compared along with the gel electrode and the result demonstrated that the IJP electrode with a diameter of 21, 19, and 16 mm shows almost similar performance as the gel electrode. Considering ECG signal quality, IJP electrode with a diameter of 19 mm was the optimal size. These IJP dry electrodes can be usable in ECG wearable as it is flexible, reusable, and can be used for a long time.

Index Terms—Dry electrodes, ECG monitoring, flexible, inkjet printing (IJP), silver nanoparticle ink, wearable sensors.

# I. INTRODUCTION

ELECTROCARDIOGRAPHY is the standard, fastest, and simplest clinical method to assess cardiovascular conditions by producing an electrocardiogram (ECG/EKG). ECG records the strength and timing of the electrical activity of the cardiovascular system, which is captured by the electrodes

Manuscript received 3 February 2023; accepted 19 February 2023. Date of publication 8 March 2023; date of current version 31 March 2023. This work was supported by the National Science Foundation (NSF) under Grant CNS-1932281. The associate editor coordinating the review of this article and approving it for publication was Prof. Huang Chen Lee. (Corresponding author: Mst Moriom Rojy Momota.)

This work involved human subjects or animals in its research. Approval of all ethical and experimental procedures and protocols was granted by the Institutional Review Board at Texas Tech University under Application No. IRB2020-783.

Mst Moriom Rojy Momota and Bashir I. Morshed are with the Department of Computer Science, Texas Tech University, Lubbock, TX 79409 USA (e-mail: mmomota@ttu.edu; bmorshed@ttu.edu).

Tamanna Ferdous and Tomoko Fujiwara are with the Department of Chemistry, University of Memphis, Memphis, TN 38152 USA (e-mail: tferdous@memphis.edu; tfjiwara@memphis.edu).

Digital Object Identifier 10.1109/JSEN.2023.3250103

placed on the skin. Due to cardiac muscle depolarization followed by repolarization during each cardiac cycle, small electrical changes occurred, which are detected by ECG electrodes [1], [2], [3], [4], [5], [6]. ECG is a low-frequency signal ranging from 0.5 to 100 Hz, typically recorded in a graph of voltage versus time showing each phase of the electrical signal. Each cardiac cycle is familiar as the heartbeat equivalent to each wave of ECG signal.

In the early days, ECG monitoring devices had vacuum tubes and water buckets, which made them larger and non-portable [2], [3]. ECG monitoring devices are now advanced, small, lightweight, portable, and comfortable. Patients can now monitor their heart activity outside of the hospital or clinic under various environmental conditions, which happened with the evaluation of technology [2], [3], [4]. Without a reliable ECG recording, it is not possible to achieve an accurate diagnosis. A proper skin–electrode contact can provide a good quality ECG signal for a reliable recording, and therefore, it is important to be careful when selecting electrodes [5], [6], [7], [8], [9], [10], [11]. For long-term remote

monitoring, an appropriate biopotential electrode is needed considering the signal quality and user comfortability. For physiological signal monitoring wet electrodes, semidry electrodes and dry electrodes are commonly used [7]. To obtain a proper electrical connection between the skin and the silver/silver chloride (Ag/AgCl) layer, a conventional wet electrode contains an electrolytic gel [8]. Although the clinically used wet gel electrode is considered the standard electrode, this electrode is disposable and is not suitable for long-term physiological signal monitoring as the gel dries out over time, which degraded the signal quality [9], [10], [35], [36], [37]. Erickson et al. [38] demonstrated that signal quality was frequently wet electrode signal quality, which was frequently seen to slightly deteriorate over the course of a 2-3-h experiment because of the adhesion mechanism results in decreasing skin-electrode impedance over time. Wet gel electrode is not comfortable for the user as skin irritation might occur because gel and skin preparations are needed such as removing hair and cleaning the skin with alcohol, before placing the electrodes. Contact and noncontact dry electrodes can be used to mitigate the discomfort of using wet gel electrodes, but the noncontact electrode captured biopotential signal has artifacts as it is capacitively coupled to the skin [11], [12], [13].

Development toward contact dry electrodes are promising and researchers are getting the same quality biopotential signal compared to wet gel electrode using dry contact electrode [14], [15]. A dry long-term monitoring ECG electrode was fabricated using carbon nanotube (CNT)/polydimethylsiloxane (PDMS), which was compatible with both conventional ECG and wearable devices [16]. A hydrophobic dry ECG electrode was developed with a mixture of carbon black powder (CB) and PDMS for both dry and water-immersed conditions [17]. PEDOT:PSS-based dry textile was reported for wearable ECG monitoring [18].

The recent focus on sensor development is to make it flexible, reusable, low cost, and give the user more comfort, which is proof of the growing market demand for flexible electronics devices [19], [20]. To make the medical service more efficient, fully flexible dry contact ECG electrodes would be promising in terms of user comfortability, sensor reusability, and long-term use for long-term ECG monitoring [21]. For microelectronics fabrication, inkjet printing (IJP) is the lowcost promising technique [22], [23]. Inkjet-printed electrodes were developed using copper and silver material on plastic and tattoo paper substrates, respectively, for ECG monitoring in personalized and ubiquitous healthcare [24]. Our research laboratory previously fabricated flexible electronics low-cost IJP respiration sensor and ECG electrode using three types of ink (25% silver, 40% silver, and 35 polypyrroles) on paper and polyimide substrate [25], [26]. We investigated gel electrode performance degraded over time by comparing gel, metal, and IJP electrode performances at the beginning of data collection and after 9 h of data collection [26]. Our fabricated IJP electrodes were stable until 9 h; on the contrary, gel electrode performance degraded over time. We also developed an ultralow-power inductively coupled wearable ECG sensor with inkjet-printed dry electrodes, where IJP electrodes were printed on paper using Ag nanoparticle ink [27]. Long-duration IJP dry electrodes in that sensor provide us long time usability. In this study, we developed ECG electrodes and optimize electrode size and shape, as the electrode–skin impedance is directly related to the interfacial area. We fabricated flexible, reusable, low-cost, long-time usable ECG electrodes in different shapes and various interfacial areas using the IJP technology with Ag B40G and Ag A211 conductive material. We also used a custom-made PVP nonconductive material for the insulation layer. We collected real-time Lead I ECG using our fabricated IJP electrodes along with the commercial gel electrode and compared the electrode's performance. For feasibility testing, we changed the position of the electrode and collect data at different activities such as resting, standing, and walking. In this work, we aimed to minimize the area size of the IJP electrodes without compromising the signal quality.

#### II. MATERIALS AND METHODS

# A. Inks

Electrodes were fabricated using JS-B40G and JS-A211 silver nanoparticle ink (manufactured by Novacentrix Inc., USA) for conductive layer printing and a custom-made poly (4-vinylphenol) (PVP) ink for insulation layer printing. JS-B40G silver nanoparticle ink contains 40% silver nanoparticle by weight, where the silver concentration is 30%–60% with 0%–20% diethylene glycol monobutyl ether solvent. The viscosity of this ink is 8-12 cP at 25 °C resulting in a surface tension of 28-32 dyne/cm. The Z-avg particle size of JS-B40G ink is 60-80 nm with a specific gravity of 1.56 (Metalon<sup>1</sup> JS-B40G datasheet, Novacentrix Inc.). JS-A211 silver nanoparticle ink also contains 40% silver nanoparticle by weight, where the silver concentration is 25%–45% with 10%-40% diethylene glycol solvent, which made this ink more adhesion to the substrate. At 25 °C, the viscosity of this ink is 8-12 cP and the surface tension is 28-32 dyne/cm. With the specific gravity of 1.6, the Z-avg particle size of JS-A211 ink is 30-50 nm (Metalon JS-A211 datasheet, Novacentrix Inc.). A custom PVP ink was used for printing the insulation layer. This PVP ink was prepared in three steps. In the first step, the ink was formulated using a mixture of dissolved 5% wt PVP powder (Sigma Aldrich 436216) and 0.77% wt., Poly (melamine-co-formaldehyde) (Sigma Aldrich 418560). Then, in the second step, the mixture was dissolved in hexanol (Sigma Aldrich 471402). As a final step, a bath-type sonicator was used for  $\sim$ 20 min to disperse the PVP until the solution turned transparent and the boiling point of this ink is 118 °C.

### B. IJP Process

A PC-controlled Dimatix Materials Printer (DMP-2850, FujiFilm Inc., USA) was used to fabricate the IJP ECG electrodes in different shapes and area sizes on polyimide substrates. This printer has MEMS-based printer cartridge with 16 printing nozzles that are arranged linearly at 254-μm spacing. The number of printing nozzles can be selected based on printing requirements. In the Dimatrix drop manager application, the cartridge temperature can be controlled by setting the nozzle head temperature. Printing platen temperature can also be increased up to 60 °C. By using the fiducial camera,

<sup>&</sup>lt;sup>1</sup>Registered trademark.

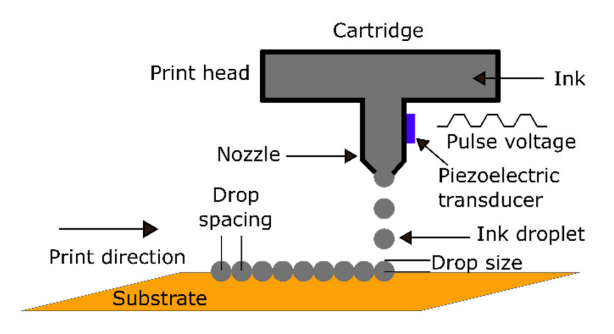


Fig. 1. IJP fabrication process showing the relation between ink droplet, drop spacing, and printing direction.

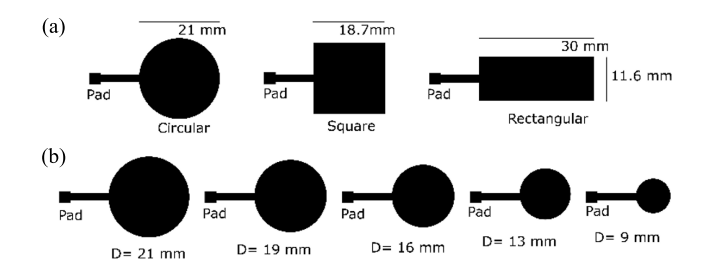


Fig. 2. (a) Layouts of IJP electrodes in circular, square, and rectangular shapes with 348-mm<sup>2</sup> area. (b) Layouts of IJP electrodes with diameters 21, 19, 16, 13, and 9 mm.

we can visually monitor the ink jetting and printed pattern in the Dimatrix drop manager application.

Fig. 1 shows the IJP fabrication process and the relation between, ink droplet, drop spacing, and printing direction.

In the IJP process, the ink is ejected from the cartridge nozzle drop by drop in the left-to-right printing direction for this printer. In the IJP process, the volume and speed of ink droplets are related to the piezoelectric actuation, which is controlled by pulsating voltages, waveforms, jetting frequencies, jetting height, meniscus setpoint, and the size of the nozzle.

# C. IJP Electrodes Layouts

As ECG electrodes' performances are dependent on electrode interfacial area to compare our fabricated electrodes' performance accurately with commercial gel electrode (Red Dot Electrodes 2560, 3M, Maplewood, MN, USA), we keep our circular, square, and rectangular electrodes size the same as 3M red dot 2560 gel electrode's size, which is 348 mm<sup>2</sup>. The first electrodes are designed in a circular, square, and rectangular shape with an area size of 348 mm<sup>2</sup>, which is shown in Fig. 2(a). To find out the optimum area size of the IJP ECG electrodes without compromising the ECG signal quality, we designed our electrode's area size to decrease by 20%, 40%, 60%, and 80% of 348 mm<sup>2</sup>. Fig. 2(b) shows the layout of the IJP electrodes with area size  $348 \text{ mm}^2$  (D = 21 mm), 278 mm<sup>2</sup> (D = 19 mm), 209 mm<sup>2</sup> (D = 16 mm), 139 mm<sup>2</sup> (D = 13 mm), and 70 mm<sup>2</sup> (D = 9 mm). In the layouts, we can see that in our ECG electrode design, the electrode is connected to a 3 × 3 mm pad through a trace where the trace is 10 mm long and 2 mm wide. Pad is used in this design to connect the wire to the electrode.

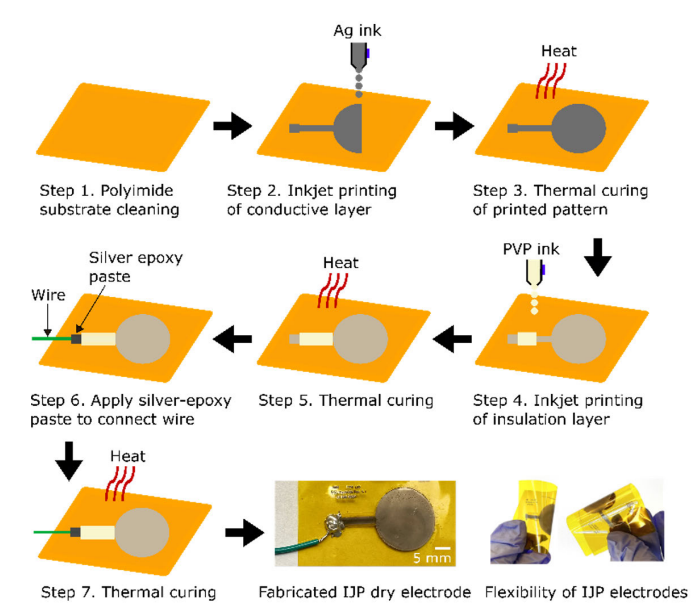


Fig. 3. Schematic of IJP electrode's fabrication process through steps 1–7. After step 7, the image of our fabricated IJP electrode and flexibility of IJP electrodes.

#### D. IJP Electrodes Fabrication Process

A DMP-2850 printer with a 10-pL DMP cartridge was used for our IJP ECG electrode fabrication. During printing, our cartridge head angle was set at  $3.4^{\circ}$ , which resulted in 15- $\mu$ m drop spacing with 1693-dpi printing resolution. We kept the platen and the cartridge at room temperature. All 16 printing nozzles of the cartridge were used during printing. The jetting voltage was 25 V for both silver nanoparticle and PVP inks.

The schematic of our IJP electrode fabrication process is shown step by step in Fig. 3. A polyimide substrate was used for our IJP electrode fabrication. First, we cleaned the substrate with isopropyl alcohol to remove any dust from it. Then, using a DMP printer, silver nanoparticle ink was injected into the substrate to fabricate the conductive layer, which is shown in step 2 of Fig. 3. The circular, square, and rectangular shape IJP electrodes conductive layer was fabricated using Ag B40 ink deposition on a 50- $\mu$ m-thin polyimide substrate. Electrodes with a diameter of 21-, 19-, 16-, 13-, and 9-mm conductive layer fabrication were performed using Ag A211 ink deposition on a 25-\mu m-thin polyimide substrate. After printing the conductive layer, in the next step, we cured it in an oven. We performed thermal curing using a Thermo Scientific Heratherm Oven (Thermo Fisher Scientific Inc., MA, USA). Silver B40 printed electrodes were cured at 250 °C for 15 min as it is a high-curing temperature ink. The minimum curing temperature of Ag B40 is 180 °C, while Ag A211 ink was cured at 200 °C temperature for 30 min.

For precise comparison of electrodes area with diameters of 21, 19, 16, 13, and 9 mm, the trace area was covered with nonconductive material PVP to avoid adding a 20-mm<sup>2</sup> trace area. For insulation layer printing, the trace width and length were 4 and 10 mm, respectively. Steps 4 and 5 of Fig. 3 illustrate the printing and curing of PVP ink for the insulation layer, respectively. Three coatings of PVP were printed and

TABLE I								
SUBJECTS INFORMATION								

Subject	Age	Gender	Height	Weight	BMI
No.			(cm)	(lb)	
1	29	Female	162.56	119	20.4
2	28	Male	182.88	198	26.9
3	29	Female	160.02	143.3	25.3
4	29	Male	172.72	154.3	23.4
5	27	Female	154.94	130	26.4

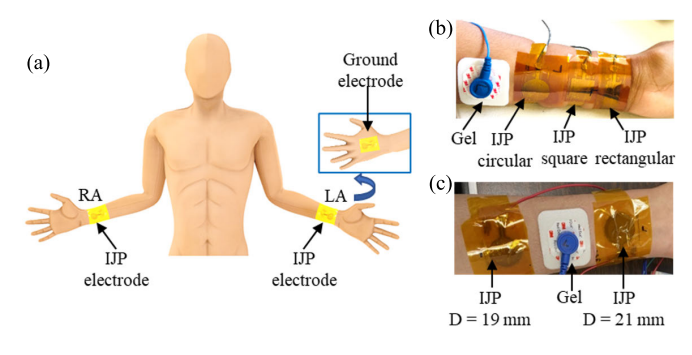


Fig. 4. (a) Schematic of Lead I electrode placement for data collection. (b) GeI, IJP circular, IJP square, and IJP rectangular electrodes are placed in the arm for data collection. (c) GeI and IJP electrodes with diameters of 21 and 19 mm are placed in the arm for data collection.

then cured at 180 °C temperature for 1 h. High-conductivity silver epoxy paste (Model: 8331DTM, MG Chemicals) was used to connect wires to the IJP electrode pads. 8331-A, and 8331-B was mixed properly in equal amount and then applied it. After applying silver epoxy, we cured it at 100 °C for 1 h to make the wire connection stable. Fabricated IJP dry electrodes are shown after step 7 of the fabrication process. By pinching electrodes between fingers, the flexibility of these electrodes is demonstrated.

# E. ECG Data Collection

- 1) Subjects: For this study, we have collected data from five healthy volunteers. All volunteers consented to be subjects of the experiment. This study protocol was approved by the Institutional Review Board (number: IRB2020-783) at Texas Tech University. Table I contains the information of the subjects such as age, gender, height, weight, and BMI.
- 2) Equipment: Commercial gel electrodes (Red Dot Electrodes 2560, 3M, Maplewood, MN, USA), and our fabricated inkjet-printed flexible dry ECG electrodes in different shapes and different diameters are used in Lead I ECG data collections. For the hardware setup, we have used Arduino Uno, AD8232, a breadboard, and jumper wires. AD8232 is a single lead ECG sensor manufactured by Sparkfun electronics.
- 3) Protocol: We used Lead I ECG placement for data collection. We placed all the test data collected simultaneously using a 3M red dot gel electrode and our IJP electrodes for accurate performance comparison. Fig. 4(a) shows the electrode placements for our Lead I ECG data collection. We place our electrodes in the left arm (LA) and the right arm (RA), and the reference electrode was placed in the hand. Fig. 4(b) and (c) shows that gel and IJP electrodes are attached to the LA arm for data collection.

# F. Statistical and Temporal Analyses

For statistical analysis, signal-to-noise ratio (SNR), kurtosis, and skewness were calculated from our collected ECG data.

1) SNR: It is the ratio of signal power to noise power. For calculating SNR, we used the following equation:

$$SNR = 20 \log_{10} \frac{A_{\text{signal}}}{A_{\text{noise}}} \tag{1}$$

where  $A_{\text{signal}}$  is the rms amplitude of the signal and  $A_{\text{noise}}$  is the rms amplitude of noise [28]. A low-pass filter with a cutoff frequency of 15 Hz was used to eliminate high-frequency noise such as powerline noise (60 Hz) and motion artifact noise (20–1000 Hz), which is a common type of noise for ECG signals [29], [30], [31], [32]. To calculate the noise present in the raw ECG signal, we subtracted the filtered signal from the raw signal. Then, we calculated the SNR using (1).

2) Kurtosis and Skewness: This statistical measurement describes how heavily the tails of distribution differ from the tails of a normal distribution [32], [33]. To measure the lack of symmetry in the distribution of the data, we have used skewness. We have calculated the kurtosis and skewness by the following equations:

Kurtosis = 
$$\frac{1}{n} \sum_{i=1}^{N} \left( \frac{\sum_{i=1}^{n} (x_i - \overline{x})^4}{s^4} \right)$$
 (2)

Skewness = 
$$\frac{1}{n} \sum_{i}^{N} \left( \frac{\sum_{i=1}^{n} (x_i - \overline{x})^3}{s^3} \right)$$
(3)

where n is the sample size and  $\overline{x}$  and s are the mean and standard deviation of the samples, respectively.

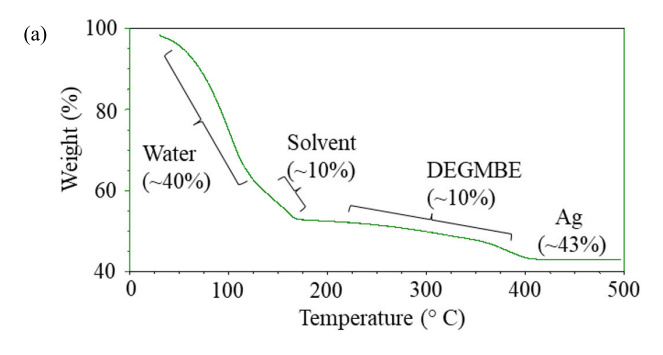
For temporal analysis, we calculated IBI, BPM, SDNN, and PNN50.

- 3) Inter-Beat Intervals (IBI): It is a segment that represents time (ms) between adjacent R-R intervals.
- 4) Beat Per Minute (BPM): It is the total number of heart-beats in 1 min.
- 5) SDNN: It is the standard deviation of normal-to-normal beat intervals, which is also referred to as the standard deviation of IBI.
- 6) PNN50: It is defined as the average number of consecutive normal sinus (NN) intervals that change more than 50 ms.

#### III. RESULTS AND DISCUSSION

# A. Ink Characterization

Thermal behavior, particle size, and contact angle of the ink droplets on the polyimide film surface were analyzed for B40 silver nanoparticle ink. Thermogravimetric analysis (TGA) revealed that the dried temperature for B40 ink is 400 °C [see Fig. 5(a)]. After cooling from 500 °C, silver B40 crystallized. The nanoparticle size measured by dynamic light scattering (DLS) displayed bimodal peaks with ~10 and 70–100-nm average diameters for B40 silver ink [see Fig. 5(b)]. The ink affinity on the flexible polyimide (PI) substrate was evaluated by measuring the contact angle of the ink droplets. Silver droplets showed extremely small contact angles on PI substrates indicating good printability [see Fig. 5(c)].



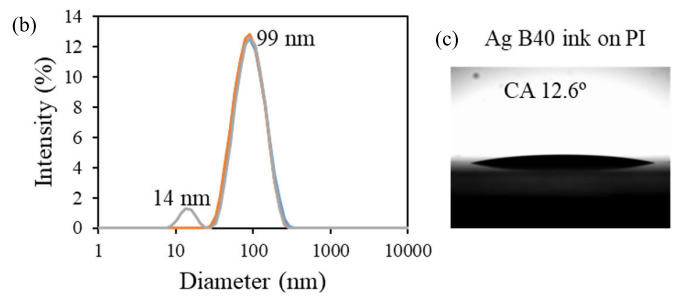


Fig. 5. Measurement of the ink droplets on the polyimide film surface. (a) TGA for thermal behavior analysis, (b) nanoparticle size measured by DLS, and (c) contact angle measured the ink affinity on the polyimide (PI) substrate.



Fig. 6. Fabricated IJP circular electrodes using B40 silver ink in different shapes: (a) circular, (b) square, and (c) rectangular.

#### B. Fabricated IJP Electrodes

Fig. 6 shows the fabricated ECG electrodes in circular, square, and rectangular shapes fabricated using silver B40 nanoparticle inks. The sheet resistance of these electrodes was measured using Ossila, a four-point probe system for sheet resistance measurement (Ossila Ltd., Sheffield S4 7WB, U.K.) The sheet resistance of IJP ECG electrodes with B40 conductive layer in circular, square, and rectangular shapes was  $40 \pm 5 \ \text{m}\Omega/\text{sq}$ .

Fabricated ECG electrodes of different area sizes with silver A211 conductive layer and the PVP insulation layer are shown in Fig. 7. The sheet resistances of these electrodes were  $15.8 \pm 3$  m $\Omega$ /sq with silver A211 conductive layer. The conductive trace of these electrodes was covered with a printed PVP insulation layer, which made the interfacial side of the trace nonconductive.

#### C. ECG Data Analysis of Collected Data

Five seconds of raw ECG signals of our collected data are shown in Fig. 8, which were collected using gel electrodes and IJP electrodes in circular, square, and rectangular shapes simultaneously. By visualization, the ECG signal of all four electrodes was similar, and therefore, we performed statistical, spectral, and temporal analysis to find the shape effect on ECG signal quality. The spectrogram is a popular way

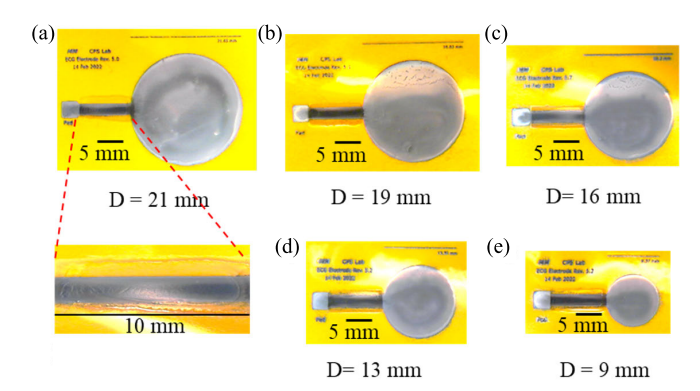


Fig. 7. Fabricated IJP circular electrodes using A211 silver ink in different diameters: (a) 21 mm, (b) 19 mm, (c) 16 mm, (d) 13 mm, and (e) 9 mm. An insulation layer was printed using PVP ink on the trace to make it nonconductive.

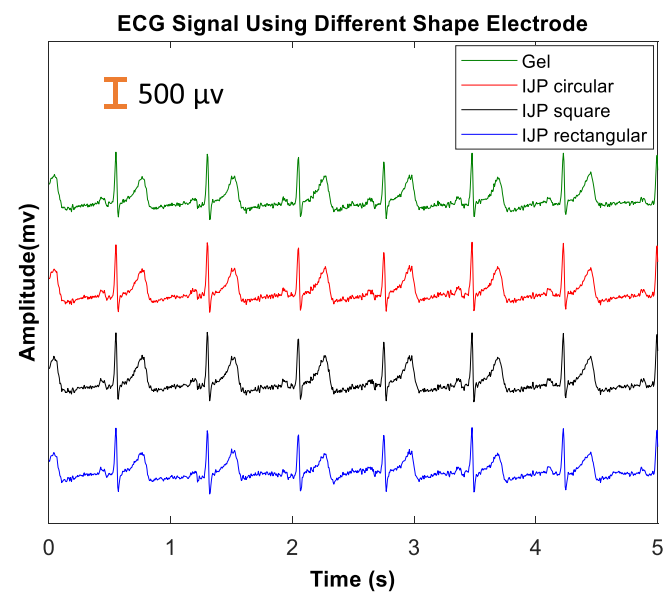


Fig. 8. Raw ECG signal collected using gel electrodes and IJP electrodes in circular, square, and rectangular shapes with Ag B40 ink conductive layer.

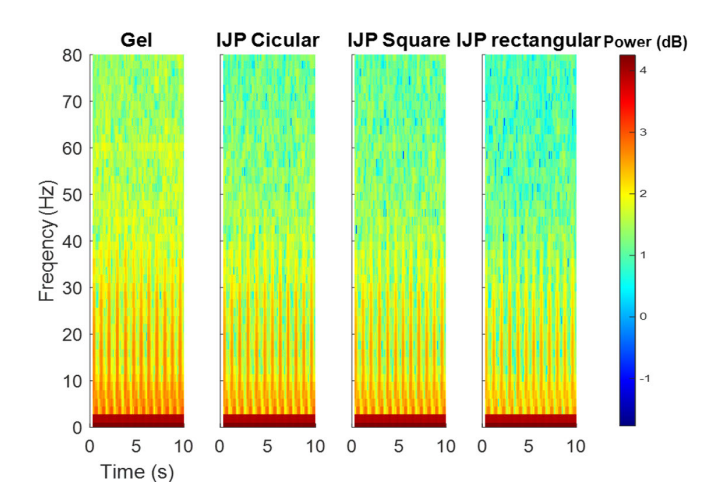


Fig. 9. Spectrogram of ECG signal collected using circular, square, and rectangular IJP electrodes and gel electrodes.

to show a time-frequency analysis from which we observe signal strength, and magnitude square coherence provides

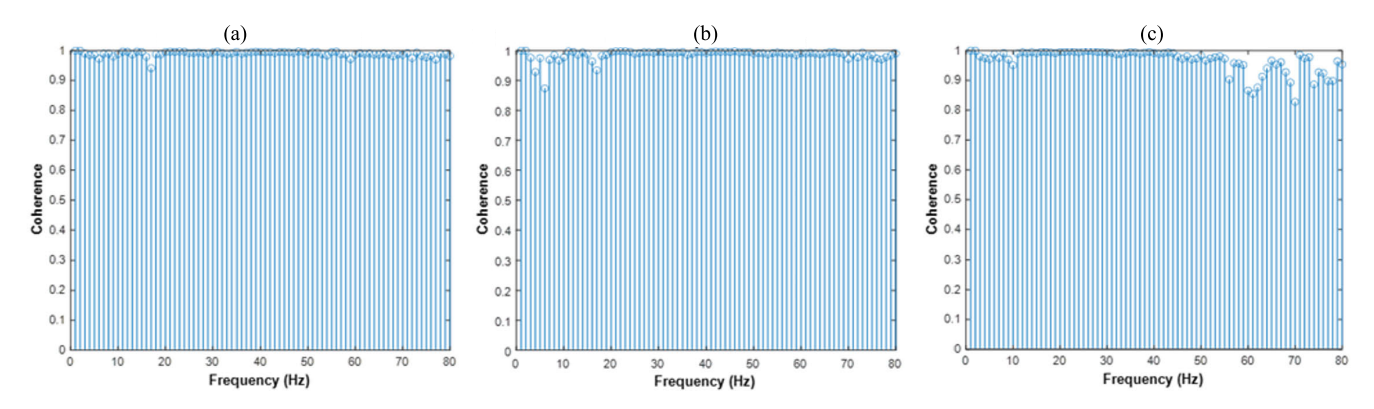


Fig. 10. Magnitude square coherence to gel electrodes of different shapes electrodes: (a) gel versus IJP circular, (b) gel versus IJP square, and (c) gel versus IJP rectangular.

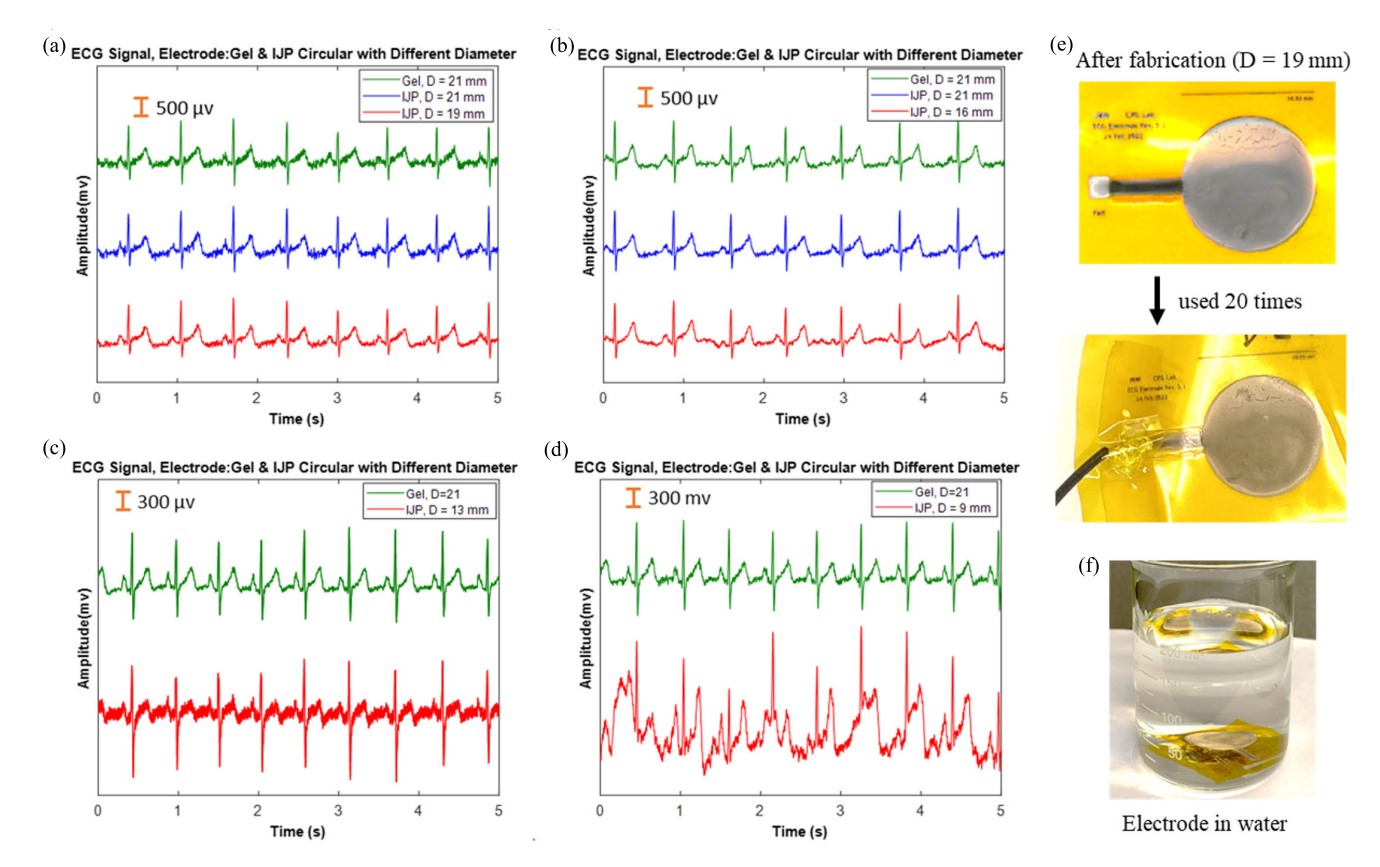


Fig. 11. Raw ECG signal collected using gel electrode and our fabricated IJP electrode in different diameters: (a) IJP D=21 mm, IJP D=19 mm, (b) IJP D=21 mm, IJP D=16 mm, (c) IJP D=13 mm, and (d) IJP D=9 mm. (e) Example of reusability of IJP electrodes. (f) Water test of IJP electrode.

information regarding the correlation between IJP and gel electrode performance.

Fig. 9 represents the spectrogram of our collected ECG data using gel and different shapes of IJP electrodes. The color bar represents the signal strength in dB. The spectrogram resulted in the signal strength of the IJP rectangular electrode being weaker than other electrodes. IJP rectangular and IJP circular signal strength was almost the same as gel electrode signal strength. Gel electrodes captured 60-Hz powerline noise than at the beginning of data collection, while IJP electrodes did not capture powerline noise, which is shown in Fig. 9.

To analyze the similarity between two signals over frequency, magnitude square coherence was calculated between the gel electrode and our fabricated IJP electrodes in different

TABLE II
PERFORMANCE ANALYSIS FOR DIFFERENT SHAPES OF ELECTRODE

Domain	Parameters	Gel	IJP	IJP	IJP
			Circular	Square	Rectangular
Statistical	SNR (dB)	21.86	22.03	21.04	21.58
Measure	Kurtosis	6.21	6.56	6.23	6.3
	Skewness	1.69	1.72	1.71	1.48
Temporal	IBI	731	731	731	731
Measure	BPM	81	81	81	81
	SDNN	76	76	76	75
	PNN50	0.15	0.15	0.15	0.17

shapes, which is shown as a plot in Fig. 10(a)–(c). To implement this plot, we used the mscohere function in MATLAB.

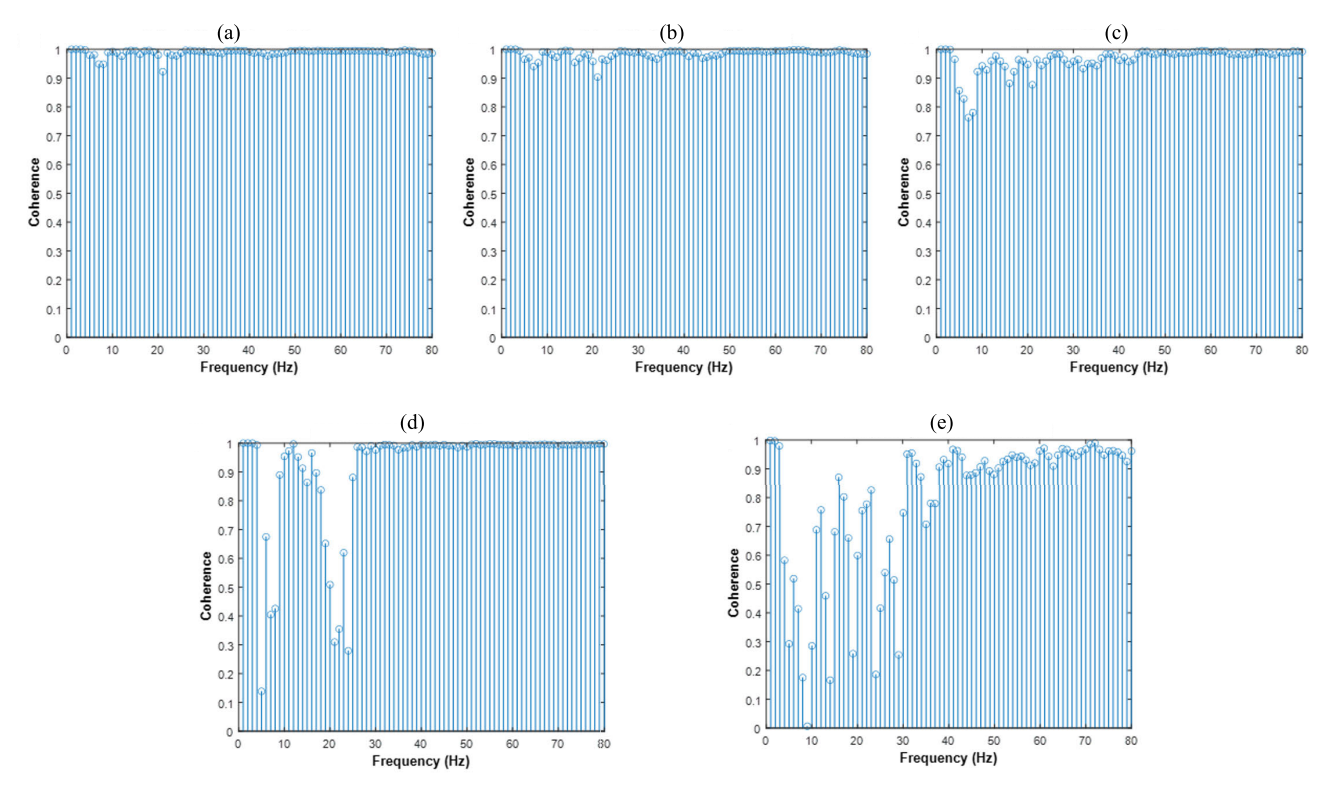


Fig. 12. Magnitude square coherence with respect to gel electrode of different diameter electrodes: (a) gel versus IJP, D=21 mm, (b) gel versus IJP, D=19 mm, (c) gel versus IJP, D=16 mm, (d) gel versus IJP, D=13 mm, and (e) gel versus IJP, D=9 mm.

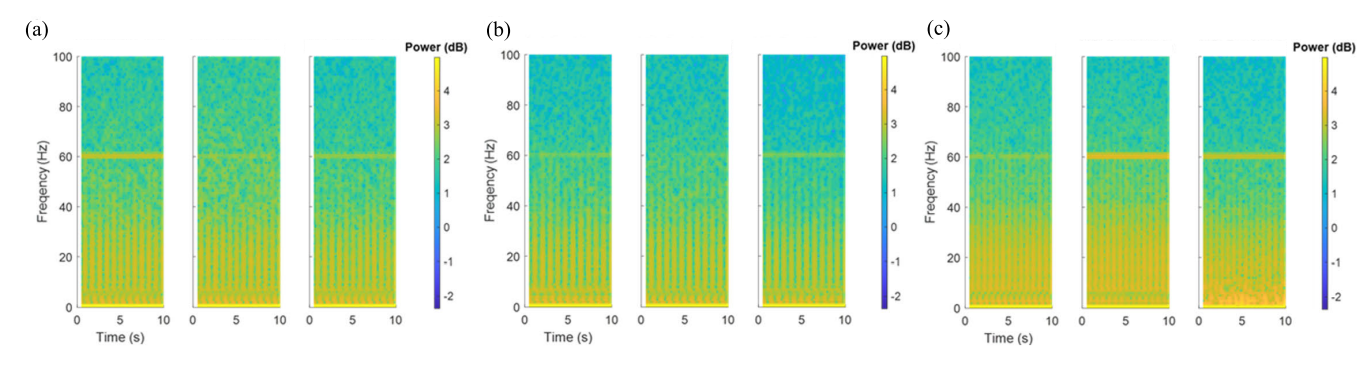


Fig. 13. Spectrogram of gel electrodes and IJP electrodes fabricated in different diameters: (a) Gel and IJP, D = 21 mm, and IJP, D = 19 mm. (b) Gel and IJP, D = 21 mm, and IJP, D = 16 mm. (c) Gel and IJP, D = 13 mm, and IJP, D = 9 mm.

Magnitude square coherence provides a result between 0 and 1, where 0 represents the lowest coherence and 1 is considered the highest coherence. Compared to IJP square and IJP rectangular, the signal of IJP circular was more coherent as, for 0-80-Hz frequency, coherence was 1. IJP square electrodes captured low-frequency noise, which is the most troublesome noise known as muscle artifacts or EMG noise that occurred due to muscle electrical activity [33]. The frequency range of EMG noise is from 1 to 15 Hz. IJP rectangular electrodes inducing more high-frequency noise such as electrode motion artifact (EMA) noise ranging between 20 and 1000 Hz occurred due to the electrode motion as rectangular electrode has larger corner and attachment at the edge of hand [39]. In terms of shape, IJP circular shape electrode is more promising as it captures less EMG and EMA noise.

Statistical and temporal measurements of gel electrodes and our fabricated IJP electrodes in three shapes are contained in Table II. IJP circular electrode achieved the highest SNR (22.03 dB) than other shapes electrodes and gel electrode. Le et al. [32] investigated dry electrode signal quality that the ECG signal with high kurtosis is less noisy. Kurtosis and skewness are calculated using the MATLAB statistical analysis toolbox. In our study, IJP circular kurtosis is highest at 6.56. We used the PySiology python package for temporal analysis. As all the data are collected at the same time IBI and BPM are the same for all electrodes. There is no significant difference between SDNN and PNN50.

The example ECG signals of our collected data using gel electrodes and our fabricated IJP electrodes in different diameters in circular shape are plotted in Fig. 11(a)–(d). We presented reusability [see Fig. 11(e)] and water test [see

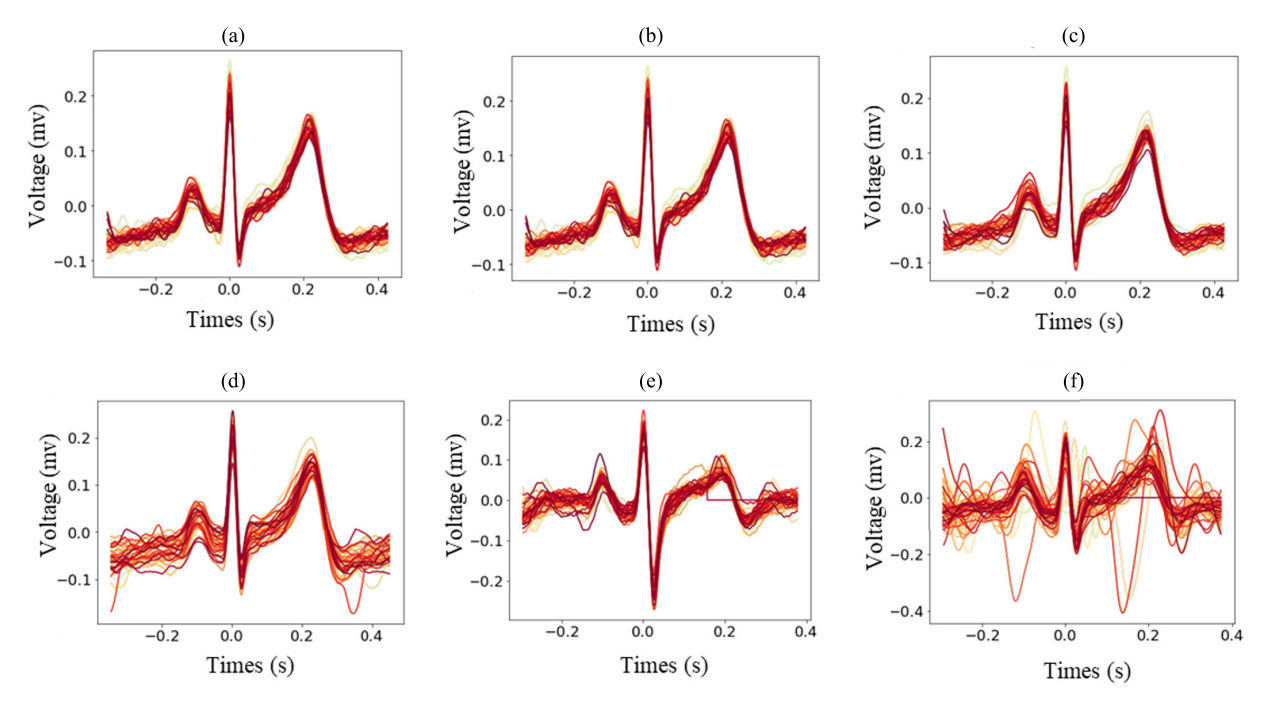


Fig. 14. Segmented heartbeat plot using different diameter electrodes: (a) Gel, D = 21 mm, (b) IJP, D = 21mm, (c) IJP, D = 19 mm, (d) IJP, D = 16 mm, (e) IJP, D = 13 mm, and (f) IJP, D = 9 mm.

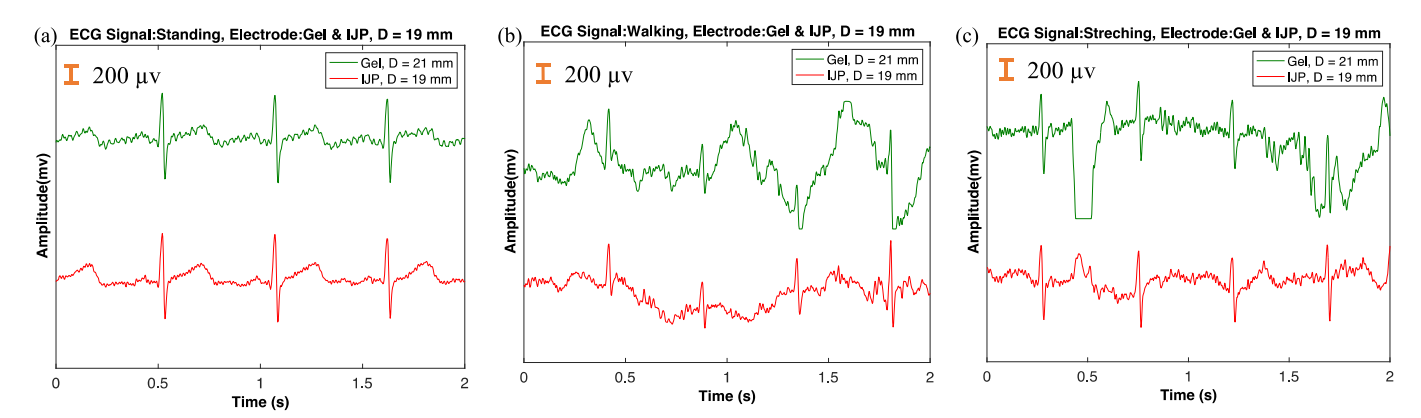


Fig. 15. Raw ECG signal in different activities using gel electrode and IJP electrode: (a) subject was in standing position, (b) subject was walking, and (c) subject was doing body stretching.

Fig. 11(f)] of IJP electrodes. Fig. 11(a) and (b) resulted that the IJP electrode with a diameter of 21, 19, and 16 mm shows similar ECG signals as the gel electrode signal. The ECG signal was collected using the IJP electrode with a diameter of 13 and 9 mm, providing poor quality ECG signal [see Fig. 11(c) and (d)]. IJP electrode with a diameter of 9 mm is too small to capture the ECG signal properly [see Fig. 11(d)]. An electrode just after the fabrication image and after 20× used image is shown in Fig. 11(e), which proves the reusability of IJP electrodes. The IJP ECG electrodes were tested for bending cycles of over 100k using a stepper motor-based test setup that did not show any degradation of IJP electrodes that proved the flexibility of IJP electrodes. Fig. 11(f) shows the water test of IJP electrodes where the IJP electrode was in the water in a beaker. Electrodes were kept in the water for one month.

Fig. 12 shows the magnitude square coherence between the gel electrode and our fabricated IJP electrodes in different

diameters. IJP electrodes with diameters of 21 and 19 mm were more coherent for 0–80-Hz frequency providing coherence close to 1 [see Fig. 12(a) and (b)]. IJP electrode with a diameter of 16 mm little bit less coherent between 5 and 15 Hz [see Fig. 12(c)]. Fig. 12(d) and (f) shows that the IJP electrodes with diameters of 13 and 9 mm showed the worst coherence in low frequencies. From Fig. 12, it is clear that, after a certain size, reducing the diameter severely impacts the performance. This can be due to the fact that the smaller size electrode does not have sufficient contact between the skin and the electrode to capture enough signal, which reduces the amount of signal propagations and increases the resistivity of the electrode leading to a weaker ECG signal.

The spectrogram analysis of different diameters of electrodes is shown in Fig. 13. Gel electrodes captured more power line noise than IJP electrodes with a diameter of 21 and 19 mm, which is visible in Fig. 13(a). Low-frequency signal strength of IJP electrodes with diameters of 21, 19, and

TABLE III

PERFORMANCE ANALYSIS OF DIFFERENT SIZE ELECTRODES

ALTERNATING ELECTRODE POSITIONS FOR LEAD I

DATA COLLECTION

Test	Electrode	Electrode	SNR	Kurtosis	Skewness
No.	Type at	Diameter	(dB)		
	position	(mm)			
	(edge,				
	middle,				
	side)				
1	Gel	21	20.94	6.48	1.59
	IJP	21	21.03	6.69	1.68
	IJP	19	21.17	6.52	1.60
2	IJP	21	21.26	6.81	1.72
	Gel	21	21.13	6.51	1.56
	IJP	19	21.68	6.70	1.48
3	IJP	19	21.59	6.54	1.74
	Gel	21	21.05	6.20	1.53
	IJP	21	21.45	6.51	1.62
4	Gel	21	20.91	6.27	1.62
	IJP	19	20.77	6.31	1.73
	IJP	21	20.91	6.78	1.81
5	IJP	21	21.32	6.71	1.83
	IJP	19	21.65	6.46	1.66
	Gel	21	20.95	6.12	1.60
6	IJP	19	21.6	6.15	1.67
	IJP	21	21.36	6.43	1.73
	Gel	21	21.08	6.04	1.51

16 mm is almost the same as gel electrode signal strength, which is visually seen in Fig. 13(a) and (b). The noise strength is stronger in ECG data collected using IJP electrodes with a diameter of 13 and 9 mm [see Fig. 13(c)].

Fig. 14 shows the segmented individual heartbeat of 20 000 samples using the NeuroKit2 python package. Segmented heartbeat collected using an IJP electrode with a diameter of 21 mm is less noisy than other electrodes [see Fig. 14(b)]. The gel electrode and the IJP electrode with a diameter of 19 mm showed an almost similar waveform [see Fig. 14(a) and (c)]. IJP electrode with a diameter of 16 mm is a little noisy [see Fig. 14(d)], but the IJP electrode with 13 and 9 mm captured a lot of noise [see Fig. 14(e) and (f)]. IJP electrodes with diameters of 21, 19, and 16 mm are showing similar individual heartbeats with less noise as gel electrodes.

Lead I data were collected using IJP electrode and gel electrodes simultaneously for accurate comparisons. We changed the electrode position alternatively and observed difference in ECG signal quality. Tests 1–6 were performed by changing the position of the gel and IJP electrode with diameters of 21 and 19 mm. A statistical measurement of changing electrode position is present in Table III. There is no significant difference due to the change of electrode positions. While the functionality is the same, gel electrode is not as durable, as comfortable as our IJP electrodes as it is sticky, causes skin irritation, and needs skin preparation for hairy skin.

The SNR of IJP electrodes with diameters of 16, 13, and 9 mm was 19.3, 16.23, and 12.8 dB, respectively. IJP electrodes smaller than 16 mm in diameter showed low signal strength. The electrode size to smaller than 16 mm was less coherent, noisy, and in some cases unable to capture the ECG

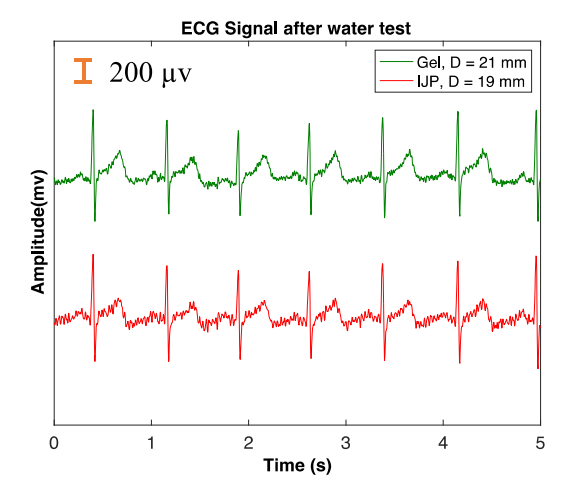


Fig. 16. Raw ECG signal collected using gel electrodes and IJP electrodes with a diameter of 19 mm after keeping IJP electrodes in water for a month.

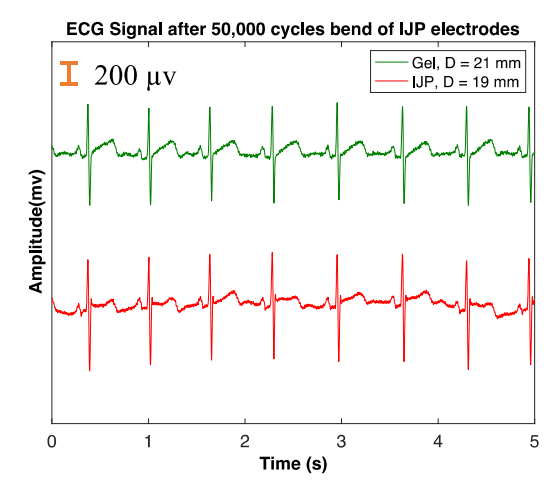


Fig. 17. Raw ECG signal collected using gel electrodes and IJP electrodes with a diameter of 19 mm after 50 000 cycles of bending of IJP electrodes.

signal properly. Fig. 15 shows the raw ECG signal when the subject was in standing, walking, and stretching positions. In a standing position compared to the gel electrode, our fabricated IJP electrode captures less noise, which is presented in Fig. 15(a). From Fig. 15(b) and (c), we can see that there is visible low-frequency oscillation when the subject was walking and doing body stretching, which is less in the case of IJP electrodes compared to gel electrodes. Due to body movements, there are motion artifacts and EMAs present in these ECG signals. In that case, our proposed IJP electrodes can be used in ECG data collection during physical activity for reliable ECG.

Fig. 16 shows the ECG signal of gel electrode and IJP electrode of diameter 19 mm. The electrode used for these data collected was kept in water for a month and then used it along with gel electrode to collect ECG data. The sheet resistance of the IJP electrode's conductive layer was  $15.8 \pm 3$  m $\Omega$ /sq just after fabrication. After keeping the IJP electrode for one month in the water, the sheet resistance changed to  $18.2 \pm 1.2$  m $\Omega$ /sq. Although there is a slight change in resistance, there is no significant difference in ECG after keeping IJP

Material	Substrate	Fabrication methods	Shape and Size	Thickness	Resistivity/ Conductivity	SNR (dB)	Reusability	Bending test	Comfort	Skin response	Ref
Copper	Polyimide	FPCB	Circular D= 2.1 cm	N/A	N/A	7.87 ± 3.36	yes	yes	yes	No reaction	[40]
CNT	PDMS	Dispersing	Circular D= 4 cm	3 mm	~1S.m <sup>-1</sup>	45.8	yes	N/A	N/A	No reaction	[16]
PEDOT:P SS	Polyureth ane(PU) nanoweb T-shirt	Screen printing	Rectangular 2 cm × 8 cm	N/A	5 Ω/sq	15.42	N/A	N/A	yes	No reaction	[41]
Silver	Tattoo paper	Inkjet printing	Circular D= 25 mm	10 μm	N/A	19.3	N/A	N/A	yes	N/A	[24]
Ag, MWCNT/ PDMS composite	PET	Screen printing	Circular D=16 mm	284.7±11. 3 μm	938.8 mS/sq	N/A	N/A	N/A	yes	N/A	[42]
Silver- plated yarns	Woven fabric	Embroideri ng	Rectangular 40 mm × 20 mm	2 mm	N/A	40.9	N/A	N/A	yes	No reaction	[43]
Silver, PVP	Polyimide	Inkjet Printing	Circular D= 19 mm	2 ± 0.5 μm	$15.8 \pm 3$ m\Omega/sq	21.68	yes	yes	yes	No reaction	Proposed

TABLE IV

COMPARISON OF OUR PROPOSED DRY ECG ELECTRODE WITH RELATED PUBLISHED ARTICLES

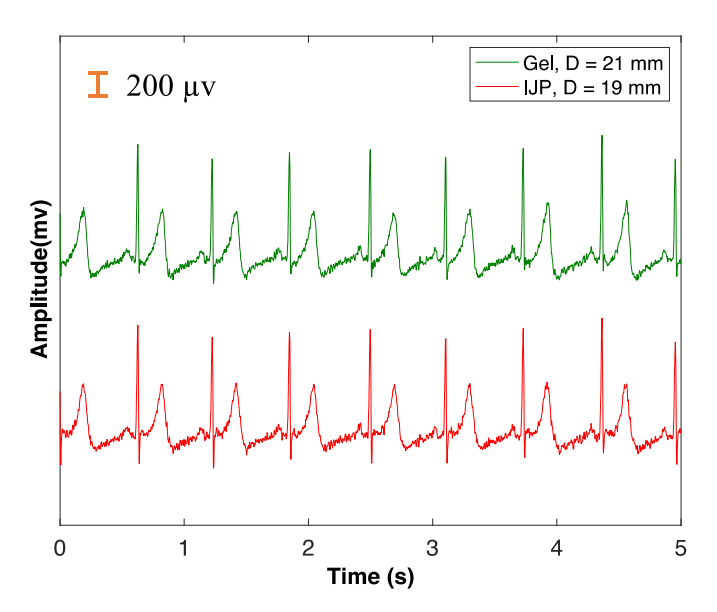


Fig. 18. Raw ECG signal collected using commercial gel electrodes and our custom IJP electrodes with a diameter of 19 mm after six months of fabrication.

electrode in water for a month, which is shown in Fig. 16. To demonstrate the durability of our IJP electrode, the ECG signal of IJP electrodes with diameter 19 mm after 50 000 bending cycles is shown in Fig. 17. IJP electrodes were bent in 10 mm diameter for 50 000 cycle times. Fig. 17 shows that the ECG signal collected using IJP electrodes after 50 000 cycles bending almost similar to gel electrodes' ECG signal.

Comparison of our fabricated IJP dry ECG electrode with related published article on dry ECG electrode is presented in Table IV. Our IJP electrode is reusable, and we also proved the durability of our electrode by performing a bending test. Our IJP electrodes did not show any skin irritation, comfortable to the users and able to capture ECG in physical activity such as walking and stretching.

Fig. 18 shows the collected raw ECG signal using gel electrodes and our fabricated dry IJP electrode with a diameter of 19 mm. Although the electrodes were used after six months of their fabrication, IJP electrodes capture similar ECG as dry electrodes.

# IV. CONCLUSION

In this work, we have fabricated dry ECG electrodes on flexible polyimide films using IJP, which is a low-cost additive manufacturing technique. IJP electrodes were fabricated in circular, square, and rectangular shapes with an area of 348 mm<sup>2</sup> using Ag B40 ink. Real-time ECG data were collected using these three shaped IJP electrodes simultaneously with gel electrodes. IJP circular and IJP rectangular electrodes were more coherent with gel electrodes. Data were collected simultaneously; therefore, there was no significant difference in temporal analysis, but in terms of SNR, kurtosis, and skewness, the IJP circular electrode was more promising than the IJP square and IJP rectangular electrodes. As ECG signal quality is dependent on the electrode's interfacial area, to come up with an optimized electrode area size for dry ECG electrodes, we have fabricated IJP electrodes with diameters of 21, 19, 16, 13, and 9 mm. For different size electrode fabrication, Ag A211 ink and a custom PVP ink were used as a conductive layer and insulation layer, respectively. We have collected real-time Lead I ECG data using different size IJP electrodes simultaneous with gel electrodes and some data were collected alternating the electrode placement. Changing electrode placement did not show any significant difference, but changing electrode size has a remarkable effect on ECG signal quality. IJP electrode with diameters of 21, 19, and 16 mm was more coherent with the gel electrode and captured less high-frequency noise. IJP electrodes with 13 and 9 mm captured more noise and were less coherent than gel electrodes. Optimizing dry ECG electrode size will be beneficial for most wearable ECG devices to make the device low-cost and small. Our fabricated flexible, reusable, low-cost IJP dry ECG electrodes can be useful for wearable and body-worn ECG monitoring devices.

#### REFERENCES

- J. A. Kaplan, B. Cronin, and T. Maus, Kaplan's Essential Cardiac Anesthesia for Cardiac Surgery, 2nd ed. Philadelphia, PA, USA: Elsevier, 2018, pp. 168–202.
- [2] Y.-L. Zheng et al., "Unobtrusive sensing and wearable devices for health informatics," *IEEE Trans. Biomed. Eng.*, vol. 61, no. 5, pp. 1538–1554, May 2014, doi: 10.1109/TBME.2014.2309951.
- [3] J. Lin et al., "Wearable sensors and devices for real-time cardiovascular disease monitoring," *Cell Rep. Phys. Sci.*, vol. 2, no. 8, pp. 1–25, Aug. 2021, doi: 10.1016/j.xcrp.2021.100541.
- [4] M. S. Lee, A. Paul, Y. Xu, W. D. Hairston, and G. Cauwenberghs, "Characterization of Ag/AgCl dry electrodes for wearable electrophysiological sensing," *Frontiers Electron.*, vol. 2, pp. 1–10, Jan. 2022, doi: 10.3389/felec.2021.700363.
- [5] Y. M. Chi, T.-P. Jung, and G. Cauwenberghs, "Dry-contact and noncontact biopotential electrodes: Methodological review," *IEEE Rev. Biomed. Eng.*, vol. 3, pp. 106–119, 2010, doi: 10.1109/RBME.2010.2084078.
- [6] A. Albulbul, "Evaluating major electrode types for idle biological signal measurements for modern medical technology," *Bioengineering*, vol. 3, no. 3, pp. 1–10, 2016, doi: 10.3390/bioengineering3030020.
- [7] G. Li, S. Wang, and Y. Y. Duan, "Towards conductive-gel-free electrodes: Understanding the wet electrode, semi-dry electrode and dry electrode-skin interface impedance using electrochemical impedance spectroscopy fitting," Sens. Actuators B, Chem., vol. 277, pp. 250–260, Dec. 2018, doi: 10.1016/j.snb.2018.08.155.
- [8] L.-F. Wang, J.-Q. Liu, B. Yang, X. Chen, and C.-S. Yang, "Fabrication and characterization of a dry electrode integrated Gecko-inspired dry adhesive medical patch for long-term ECG measurement," *Microsyst. Technol.*, vol. 21, no. 5, pp. 1093–1100, 2015, doi: 10.1007/s00542-014-2279-4.
- [9] Y.-H. Chen et al., "Soft, comfortable polymer dry electrodes for high quality ECG and EEG recording," Sensors, vol. 14, no. 12, pp. 23758–23780, 2014, doi: 10.3390/s141223758.
- [10] A. C. Myers, H. Huang, and Y. Zhu, "Wearable silver nanowire dry electrodes for electrophysiological sensing," *RSC Adv.*, vol. 5, no. 15, pp. 11627–11632, 2015, doi: 10.1039/C4RA15101A.
- [11] J. S. Lee, J. Heo, W. K. Lee, Y. G. Lim, Y. H. Kim, and K. S. Park, "Flexible capacitive electrodes for minimizing motion artifacts in ambulatory electrocardiograms," *Sensors*, vol. 14, pp. 14732–14743, Aug. 2014, doi: 10.3390/s140814732.
- [12] N. Meziane, S. Yang, M. Shokoueinejad, J. G. Webster, M. Attari, and H. Eren, "Simultaneous comparison of 1 gel with 4 dry electrode types for electrocardiography," *Physiol. Meas.*, vol. 36, no. 3, pp. 513–529, Mar. 2015, doi: 10.1088/0967-3334/36/3/513.
- [13] S. Ha et al., "Integrated circuits and electrode interfaces for noninvasive physiological monitoring," *IEEE Trans. Biomed. Eng.*, vol. 61, no. 5, pp. 1522–1537, May 2014, doi: 10.1109/TBME.2014.2308552.
- [14] S. Yao and Y. Zhu, "Nanomaterial-enabled dry electrodes for electrophysiological sensing: A review," *JOM*, vol. 68, no. 4, pp. 1145–1155, 2016, doi: 10.1007/s11837-016-1818-0.
- [15] H. Wu et al., "Materials, devices, and systems of on-skin electrodes for electrophysiological monitoring and human-machine interfaces," Adv. Sci., vol. 8, no. 2, pp. 1–30, Jan. 2021, doi: 10.1002/advs.202001938.
- [16] H.-C. Jung et al., "CNT/PDMS composite flexible dry electrodesfor long-term ECG monitoring," *IEEE Trans. Biomed. Eng.*, vol. 59, no. 5, pp. 1472–1479, May 2012, doi: 10.1109/TBME.2012.2190288.
- [17] B. A. Reyes et al., "Novel electrodes for underwater ECG monitoring," *IEEE Trans. Biomed. Eng.*, vol. 61, no. 6, pp. 1863–1876, Jun. 2014, doi: 10.1109/TBME.2014.2309293.
- [18] D. Pani, A. Dessì, J. F. Saenz-Cogollo, G. Barabino, B. Fraboni, and A. Bonfiglio, "Fully textile, PEDOT: PSS based electrodes for wearable ECG monitoring systems," *IEEE Trans. Biomed. Eng.*, vol. 63, no. 3, pp. 540–549, Mar. 2016, doi: 10.1109/TBME.2015.2465936.
- [19] S. Xu, A. Jayaraman, and J. A. Rogers, "Skin sensors are the future of health care," *Nature*, vol. 571, no. 7765, pp. 319–321, Jul. 2019, doi: 10.1038/d41586-019-02143-0.
- [20] W. Gao, H. Ota, D. Kiriya, K. Takei, and A. Javey, "Flexible electronics toward wearable sensing," Acc. Chem. Res., vol. 52, no. 3, pp. 523–533, Mar. 2019, doi: 10.1021/acs.accounts.8b00500.

- [21] A. A. Chlaihawi, B. B. Narakathu, S. Emamian, B. J. Bazuin, and M. Z. Atashbar, "Development of printed and flexible dry ECG electrodes," Sens. Bio-Sens. Res., vol. 20, pp. 9–15, Sep. 2018, doi: 10.1016/j.sbsr.2018.05.001.
- [22] Z. Yin, Y. Huang, N. Bu, X. Wang, and Y. Xiong, "Inkjet printing for flexible electronics: Materials, processes and equipments," *Chin. Sci. Bull.*, vol. 55, no. 30, pp. 3383–3407, Nov. 2010, doi: 10.1007/s11434-010-3251-y.
- [23] H. Hussin, N. Soin, S. F. W. M. Hatta, F. A. M. Rezali, and Y. A. Wahab, "Review—Recent progress in the diversity of inkjet-printed flexible sensor structures in biomedical engineering applications," *J. Electrochemical Soc.*, vol. 168, no. 7, Jul. 2021, Art. no. 077508, doi: 10.1149/1945-7111/ac0e4b.
- [24] J. C. Batchelor and A. J. Casson, "Inkjet printed ECG electrodes for long term biosignal monitoring in personalized and ubiquitous healthcare," in *Proc. 37th Annu. Int. Conf. IEEE Eng. Med. Biol. Soc. (EMBC)*, Aug. 2015, pp. 4013–4016, doi: 10.1109/EMBC.2015.7319274.
- [25] A. Mohapatra, B. I. Morshed, S. Shamsir, and S. K. Islam, "Inkjet printed thin film electronic traces on paper for low-cost body-worn electronic patch sensors," in *Proc. IEEE 15th Int. Conf. Wearable Implant. Body Sensor Netw. (BSN)*, Mar. 2018, pp. 169–172, doi: 10.1109/BSN.2018.8329685.
- [26] M. M. R. Momota and B. I. Morshed, "Inkjet printed flexible electronic dry ECG electrodes on polyimide substrates using silver ink," in *Proc. IEEE Int. Conf. Electro Inf. Technol. (EIT)*, Jul. 2020, pp. 464–468, doi: 10.1109/EIT48999.2020.9208322.
- [27] B. I. Morshed, "Ultra low-power inductively coupled wearable ECG sensor design with inkjet printed dry electrodes," in *Proc. United States Nat. Committee URSI Nat. Radio Sci. Meeting (USNC-URSI NRSM)*, Jan. 2019, pp. 1–2, doi: 10.23919/USNC-URSI-NRSM.2019.8712941.
- [28] S. Masihi et al., "Development of a flexible wireless ECG monitoring device with dry fabric electrodes for wearable applications," *IEEE Sensors J.*, vol. 22, no. 12, pp. 11223–11232, Jun. 2022, doi: 10.1109/JSEN.2021.3116215.
- [29] U. Satija, B. Ramkumar, and M. S. Manikandan, "Real-time signal quality-aware ECG telemetry system for IoT-based health care monitoring," *IEEE Internet Things J.*, vol. 4, no. 3, pp. 815–823, Jun. 2017, doi: 10.1109/JIOT.2017.2670022.
- [30] L. Smital et al., "Real-time quality assessment of long-term ECG signals recorded by wearables in free-living conditions," *IEEE Trans. Biomed. Eng.*, vol. 67, no. 10, pp. 2721–2734, Oct. 2020, doi: 10.1109/TBME.2020.2969719.
- [31] J. Pan and W. J. Tompkins, "A real-time QRS detection algorithm," *IEEE Trans. Biomed. Eng.*, vol. BME-32, no. 3, pp. 230–236, Mar. 1985, doi: 10.1109/TBME.1985.325532.
- [32] K. Le, A. Servati, S. Soltanian, P. Servati, and F. Ko, "Performance and signal quality analysis of electrocardiogram textile electrodes for smart apparel applications," *Frontiers Electron.*, vol. 2, pp. 1–11, Jun. 2021, doi: 10.3389/felec.2021.685264.
- [33] M. S. Zaman and B. I. Morshed, "Estimating reliability of signal quality of physiological data from data statistics itself for real-time wearables," in *Proc. 42nd Annu. Int. Conf. IEEE Eng. Med. Biol. Soc. (EMBC)*, Jul. 2020, pp. 5967–5970, doi: 10.1109/EMBC44109.2020.9175317.
- [34] G. Gabrieli, A. Azhari, and G. Esposito, "PySiology: A Python package for physiological feature extraction," in *Proc. Neural Approaches to Dynamics of Signal Exchanges*, A. Esposito, M. Faundez-Zanuy, F. Morabito, and E. Pasero, Eds. Singapore: Springer, Sep. 2019, pp. 395–402, doi: 10.1007/978-981-13-8950-4\_35.
- [35] G. Cosoli, S. Spinsante, F. Scardulla, L. D'Acquisto, and L. Scalise, "Wireless ECG and cardiac monitoring systems: State of the art, available commercial devices and useful electronic components," *Measurement*, vol. 177, Jun. 2021, Art. no. 109243, doi: 10.1016/j. measurement.2021.109243.
- [36] L. Zhang et al., "Fully organic compliant dry electrodes self-adhesive to skin for long-term motion-robust epidermal biopotential monitoring," *Nature Commun.*, vol. 11, no. 1, p. 4683, Sep. 2020, doi: 10.1038/s41467-020-18503-8.
- [37] R. Castrillón, J. J. Pérez, and H. Andrade-Caicedo, "Electrical performance of PEDOT:PSS-based textile electrodes for wearable ECG monitoring: A comparative study," *Biomed. Eng. OnLine*, vol. 17, no. 1, pp. 1–23, Dec. 2018, doi: 10.1186/s12938-018-0469-5.
- [38] J. C. Erickson, E. Stepanyan, and E. Hassid, "Comparison of dry and wet electrodes for detecting gastrointestinal activity patterns from body surface electrical recordings," *Ann. Biomed. Eng.*, pp. 1–12, Jan. 2023, doi: 10.1007/s10439-023-03137-w.

- [39] M. M. R. Momota and B. I. Morshed, "ML algorithms to estimate data reliability metric of ECG from inter-patient data for trustable AI-based cardiac monitors," *Smart Health*, vol. 26, Dec. 2022, Art. no. 100350, doi: 10.1016/j.smhl.2022.100350.
- [40] X. Wang et al., "Flexible non-contact electrodes for wearable biosensors system on electrocardiogram monitoring in motion," *Frontiers Neurosci.*, vol. 16, Jun. 2022, Art. no. 900146, doi: 10.3389/fnins.2022.900146.
- [41] S. K. Sinha et al., "Screen-printed PEDOT:PSS electrodes on commercial finished textiles for electrocardiography," ACS Appl. Mater. Interface, vol. 9, no. 43, pp. 37524–37528, Nov. 2017, doi: 10.1021/acsami.7b09954.
- [42] A. A. Chlaihawi et al., "Development of flexible dry ECG electrodes based on MWCNT/PDMS composite," in *Proc. IEEE Sensors*, Nov. 2015, pp. 1–4, doi: 10.1109/ICSENS.2015.7370218.
- [43] H. Liu et al., "The effect of chlorine/argentum atomic ratios on electrochemical behaviors and signal acquisition abilities of embroidered electrodes for bio-potential signal measurement," *Appl. Phys. A, Solids Surf.*, vol. 125, no. 8, pp. 1–11, Aug. 2019, doi: 10.1007/s00339-019-2793-4



Mst Moriom Rojy Momota (Graduate Student Member, IEEE) received the B.Sc. degree in electronics and telecommunication engineering from the Rajshahi University of Engineering and Technology, Rajshahi, Bangladesh, India, in 2017. She is currently pursuing the Ph.D. degree with the Department of Computer Science, Texas Tech University, Lubbock, TX, USA. She has been working as a Graduate Research Assistant at the Cyber-Physical Systems (CPS) Laboratory, Texas Tech University,

since 2020. Her research interests include flexible electronics components and sensors for CPS interface to the application of artificial intelligence (AI) to data reliability estimations.



Bashir I. Morshed (Senior Member, IEEE) received the B.Sc. degree in electrical and electronics engineering from the Bangladesh University of Engineering and Technology, Dhaka, India, in 2001, the M.Sc. degree in electrical and computer engineering from the University of Windsor, Windsor, ON, Canada, in 2004, and the Ph.D. degree in electrical and computer engineering from Carleton University, Ottawa, ON, Canada, in 2010.

He has been with the Computer Science Department, Texas Tech University, Lubbock, TX, USA, as an Associate Professor, since 2020. Previously, he has been with the Electrical and Computer Engineering Department, University of Memphis, Memphis, TN, USA, since 2011.

Dr. Morshed was a recipient of the Prestigious Canadian Commonwealth Scholarship in 2002.



Tamanna Ferdous received the M.S. degree in analytical chemistry from the University of Memphis, Memphis, TN, USA, in 2021, where she is pursuing the Ph.D. degree with the Department of Chemistry.

She is currently working both as a Graduate Teaching Assistant and a Research Assistant. Her research interests include the synthesis and modification of various polymers, and preparing biocompatible hydrogel to deliver drugs in targeted areas to treat certain diseases such as

bone cancer and bone wounds.



Tomoko Fujiwara received the Ph.D. degree in polymer science from the Kyoto Institute of Technology, Kyoto, Japan, in 2001.

She is a Professor of Chemistry with the University of Memphis, Memphis, TN, USA. The Fujiwara research group synthesizes polymers and formulates membranes, hydrogels, fibers, and nanoparticles for applications in energy devices, sensors, and biomaterials. She has authored over 80 publications in related fields.